Tracking Control for a Cushion Robot Based on Fuzzy Path Planning With Safe Angular Velocity

Ping Sun and Zhuang Yu

***Abstract*—This study proposes a new nonlinear tracking control method with safe angular velocity constraints for a cushion robot. A fuzzy path planning algorithm is investigated and a real-time desired motion path of obstacle avoidance is obtained. The angular velocity is constrained by the controller, so the planned path guarantees the safety of users. According to Lyapunov theory, the controller is designed to maintain stability in terms of solutions of linear matrix inequalities and the controller's performance with safe angular velocity constraints is derived. The simulation and experiment results confirm the effectiveness of the proposed method and verify that the angular velocity of the cushion robot provided safe motion with obstacle avoidance.**

***Index Terms*—Cushion robot, path planning, safe angular velocity, tracking control.**

I. Introduction

CURRENT trends in aging societies have increased the need for health care and rehabilitation, especially for elderly and disabled people. Motion disability seriously impedes daily life activities and incurs a large psychological burden [1]. Many researchers have endeavored to improve the lifestyles of disabled people through rehabilitation training and mechanistic aids such as robotic exoskeleton [2], wearable robots that assist lower-limb movement [3], knee joint misalignment exoskeleton [4], omnidirectional rehabilitative training walker [5], and cushion robot [6]. In most of these studies, the robots focus primarily on developing control strategies to move along a predefined path with the designed position controller. The tracking performances of these robots have been improved by various control approaches, such as fuzzy sliding mode control [7], neural network control [8], gait trajectory adaptive control [9], and guaranteed cost non-fragile tracking control [10]. However, these control methods require that the motion path has been fixed in advance. In fact, the tracking path in narrow, complex, and unknown indoor environments is not easily determined. Therefore, to reach a goal while avoiding all obstacles, a mobile robot must plan a safe motion path in real time.

Path planning and navigation strategies of mobile robots have attracted considerable attention in recent years. When a mobile robot traverses an unstructured environment, it must reach its target without colliding with obstacles in its path. Real-time path planning enables a mobile robot to move in an unknown environment using the information acquired by its sensors [11]. The path planning problem has been solved by different evolutionary methods including fuzzy logic [12], fuzzy clustering [13], the fuzzy path preview algorithm [14], adaptive neuro-fuzzy inference [15], and the directional intention distance fuzzy learning method [16]. In these approaches, the robot usually obtains the distance information between itself and nearby obstacles through its sensors, then turns at an appropriate angle to avoid the obstacles. However, the existing path planning method pays little attention to the angular velocity of obstacle avoidance. The angular velocity of the robot's motion should be sufficiently large without imposing constraints during path planning. The practical requirements of human support robots differ from those of industrial robots. For instance, a large spin speed in human support robots poses a danger to users, so the angular velocity of obstacle avoidance should not exceed the prescribed safe range. To guarantee the safety of users, the path planning in human robots must constrain the angular velocity performance.

In fact, the constraint problem is often considered in control design because any violation of the constraints can lead to performance degradation [17]. An important consideration in designing controllers in robotic systems is that it should be simple to implement in real-time [18]. At present, the performance requirements of constrained systems are met by saturation functions and barrier Lyapunov functions (BLFs) [19]−[21]. However, both of these approaches are designed for passive physical constraints and require a complex controller structure. Furthermore, the controller cannot actively restrict angular velocity of the system. To our knowledge, fuzzy path planning under restricted angular velocity has not been applied to the tracking control of human support robots.

The paper proposes a new tracking control method in which the controller restrains the spin velocity of obstacle avoidance by restricting the angular velocity performance. In many problems, theoretical study and engineering applications are equally important and should be studied together. Here we investigate a cushion robot [6]. The cushion robot and an example of its use are photographed in Figs. 1 and 2, respectively. The cushion robot moves on three omnidirectional wheels to flexibly assist elderly people moving inside a room, conveni-

Manuscript received June 8, 2016; accepted October 28, 2016. This work was supported by the Program for Liaoning Excellent Talents in University of China (LJQ2014013) and the Liaoning Natural Science Foundation of China (2015020066). Recommended by Associate Editor Wei He. *(Corresponding author: Ping Sun).*

Citation: P. Sun and Z. Yu, "Tracking control for a cushion robot based on fuzzy path planning with safe angular velocity," *IEEE/CAA J. of Autom. Sinica*, vol. 4, no. 4, pp. 610−619, Oct. 2017.

P. Sun and Z. Yu are with the School of Information Science and Engineering, Shenyang University of Technology, Shenyang 110870, China (e-mail: tonglongsun@sut.edu.cn; emailyuz@163.com).

Color versions of one or more of the figures in this paper are available online at http://ieeexplore.ieee.org.

Digital Object Identifier 10.1109/JAS.2017.7510607

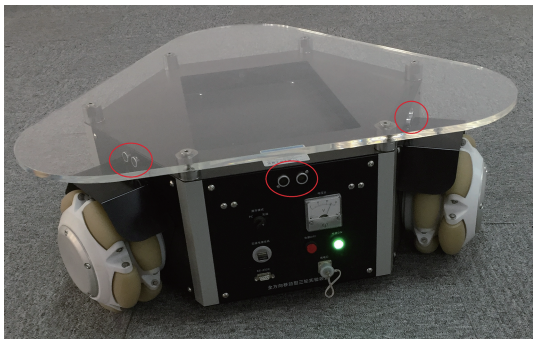

Fig. 1. Photograph of cushion robot.

Fig. 2. The cushion robot in use [6].

ently supporting their daily life activities.

Motivated by the above observations, we developed a cushion robot with several novel functionalities. The main contributions of this paper are summarized below:

1) The path planning method is proposed on the basis of fuzzy algorithm. To guarantee the user's safety, the angular velocity of obstacle avoidance is limited on the robot's turning motion. The desired motion path is obtained in real time using the output angle from starting point to goal.

2) The saturation function formulations and barrier Lyapunov function state of previous works [19]−[21] are replaced by a new tracking control method. In the proposed approach, the angular velocity constraints are imposed by the controller. Closed loop stability of the tracking error system is established by a Lyapunov function and the safe motion of the angular velocity is derived.

3) The applicability of the proposed scheme is demonstrated on a motion path of obstacle avoidance. The efficiency of tracking control with safe angular velocity is demonstrated on the cushion robot.

The remainder of this paper is organized as follows. Section II formulates the dynamic model of the cushion robot, and Section III derives the motion path of obstacle avoidance. The tracking control problem with constrained angular velocity is presented in Section IV. Simulation and experiment results are given in Sections V and VI, respectively. Conclusions are provided in Section VII.

II. Dynamics Model of the Cushion Robot

The tracking control is based on real-time motion paths of the cushion robot. The coordinates and structure of the cushion robot, from which the tracking control is derived, are shown in Fig. 3. The robot has three omnidirectional wheels controlled by three independent DC motors.

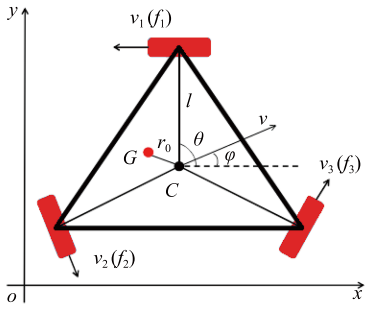

Fig. 3. Structure of cushion robot.

The variables in Fig. 3 are defined below:
$\Sigma(x, O, y)$: Absolute coordinate system;
v: Speed of the cushion robot;
v_i: Speed of an omniwheel $(i = 1, 2, 3)$;
f_i: Force on each omniwheel;
C: Center of gravity of the cushion robot;
G : Center of gravity of the load (supplied by the user);
r_0: Distance between C and G;
φ: Angle between x axis and speed v;
θ: Angle between x axis and the position direction of each omniwheel;
l: Distance between the centers of the cushion robot and the omniwheels.

The dynamics model is given by [6]

$$M_0\ddot{X}(t) = B(\theta)u(t) \tag{1}$$

where

$$M_0 = \begin{bmatrix} M+m & 0 & 0 \\ 0 & M+m & 0 \\ 0 & 0 & I_0 + mr_0^2 \end{bmatrix}$$

$$X(t) = \begin{bmatrix} x(t) \\ y(t) \\ \theta(t) \end{bmatrix}, \quad u(t) = \begin{bmatrix} f_1 \\ f_2 \\ f_3 \end{bmatrix}$$

$$B(\theta) = \begin{bmatrix} -\sin\theta & -\sin(\frac{2\pi}{3}+\theta) & -\sin(\frac{4\pi}{3}+\theta) \\ \cos\theta & \cos(\frac{2\pi}{3}+\theta) & -\cos(\frac{4\pi}{3}+\theta) \\ l & l & l \end{bmatrix}$$

where M is the mass of the cushion robot, m is the equivalent mass of the user, and I_0 and mr_0^2 denote the mass inertias of the cushion robot and m, respectively. f_1, f_2, and f_3 are the driving forces on the three omnidirectional wheels. Clearly, the system of differential equation (1) is nonlinear because the direction angle θ changes with time.

Setting

$$\begin{cases} x_1(t) = X(t) \\ x_2(t) = \dot{X}(t). \end{cases} \tag{2}$$

Equation (1) can be expressed as follows:

$$\begin{cases} \dot{x}_1(t) = x_2(t) \\ \dot{x}_2(t) = M_0^{-1}B(\theta)u(t). \end{cases} \tag{3}$$

The actual motion trajectory is $X(t)$, and the real-time planned motion trajectory is $X_d(t)$, the trajectory tracking error $e_1(t)$ and velocity tracking error $e_2(t)$ are given by

$$e_1(t) = X(t) - X_d(t) \tag{4}$$
$$e_2(t) = \dot{X}(t) - \dot{X}_d(t) = x_2(t) - \dot{X}_d(t). \tag{5}$$

The design of the control input force is

$$u(t) = B^{-1}(\theta)M_0[\ddot{X}_d(t) + K_p e_1(t) + K_d e_2(t)] \tag{6}$$

where K_p and K_d are controller parameters to be designed.

The error dynamics are then obtained as

$$\begin{cases} \dot{e}_1(t) = e_2(t) \\ \dot{e}_2(t) = K_d e_2(t) + K_p e_1(t). \end{cases} \tag{7}$$

Definition 1: Considering the system of the cushion robot (1), $\theta(t)$ is the actual angle of obstacle avoidance and $\dot{\theta}(t)$ is the actual angular velocity of the motion. In the path planning of the cushion robot, the velocity $\dot{\theta}(t)$ is regarded as safe under the condition $|\dot{\theta}(t)| \le a$, where a is a specified positive constant.

This paper designs a controller $u(t)$ under the safety constraints of $\dot{\theta}(t)$. The design simultaneously satisfies the following two requirements:

1) The trajectory tracking error $e_1(t)$ and velocity tracking error $e_2(t)$ are asymptotically stable.

2) The actual angular velocity $\dot{\theta}(t)$ satisfies

$$\left|\dot{\theta}(t)\right| \le a. \tag{8}$$

Remark 1: This study plans a path with safe angular velocity. Therefore, the tracking motion angular velocity $\dot{\theta}(t)$ is an important performance index. Equation (8) provides a simple means of restricting the angular velocity of the cushion robot.

Human support robots work in narrow environments with complex surroundings. Therefore, the cushion robot cannot be guided by a prescribed motion path. Instead, the robot's path is specially planned to avoid collisions between the robot and obstacles. The tracking of such a path is accomplished by a controller with angular velocity constraints. Fig. 4 is a block diagram of the proposed control system for the cushion robot. The following sections present the fuzzy path planning and the controller with angular velocity constraints, respectively.

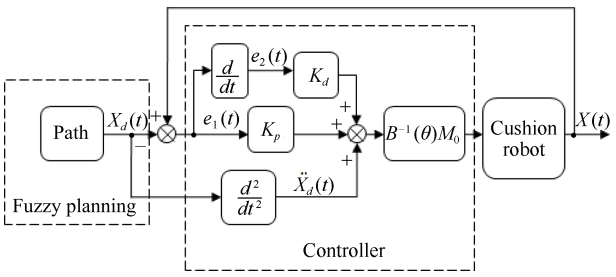

Fig. 4. Block diagram of the control system.

III. Fuzzy Path Planning

The path planning is divided into two parts: In the first part, the cushion robot searches a collision-free path based on the information gained from its sensors; in the second part, it moves towards the goal while avoiding the nearby obstacles.

A. Determination of Membership Functions and Fuzzy Set

To move within an unknown indoor environment, the robot requires a collision avoidance functionality. For this purpose, the robot considers the values of its input variables, such as the distances and direction angles between itself and the surrounding obstacles. The required inputs are the distance information of the front, left, and right obstacles (D_F, D_L, and D_R, respectively), and the direction angle A_F between the forward direction of the robot and the target point. The output A_D is the steering angle for obstacle avoidance by the cushion robot.

Without loss of generality, the membership functions in the fuzzy algorithm design can be assumed as triangular and symmetric. The inputs to the fuzzy algorithm are two distance variables with different values, namely F (far) and N (near), and five values of the direction angle. The distance values are defined as fuzzy membership functions shown in Fig. 5. The values of the direction angle are LB (left big), LS (left small), Z (zero), RS (right small), and RB (right big). Their membership functions are shown in Fig. 6. The distance and input angles to the fuzzy system determine the steering angle A_D of the robot. The steering angle is output in the form of five values assigned as TLB (left big), TLS (left small), TZ (zero), TRS (right small), and TRB (right big) (see Fig. 7).

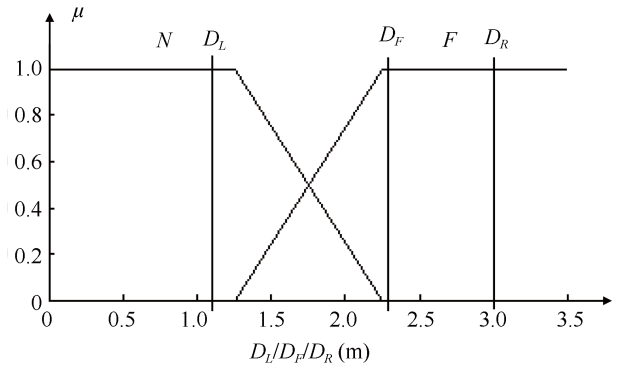

Fig. 5. Fuzzy membership functions of D_L, D_F, and D_R.

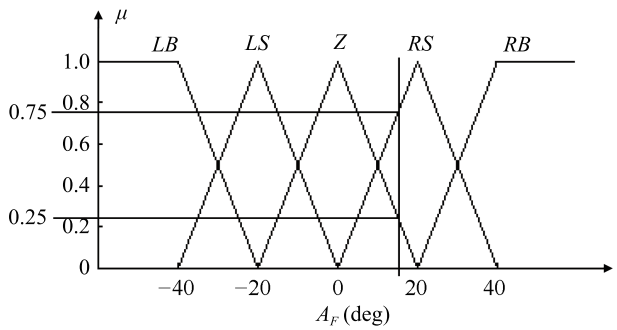

Fig. 6. Fuzzy membership functions of A_F.

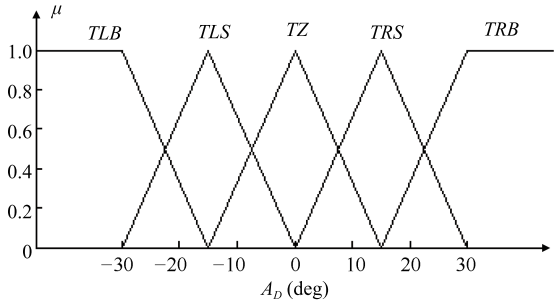

Fig. 7. Fuzzy membership functions of A_D.

B. Determination of Fuzzy Rules

The fuzzy rules are if then statements consisting of a premise and a consequent. The knowledge rule-base comprises $2^3 \times 5 = 40$ rules. When the robot perceives a left (right) target point, it turns left (right). When the frontal obstacle is close and the target point is behind the obstacle, the cushion robot selects the safer of the two turns (right or left). If the left obstacle is equidistant or further than the right obstacle, the cushion robot makes a left turn; otherwise, it turns right. Once all of the nearby obstacles have been avoided, it moves straight toward the target. As an example, an obstacle is placed to the left of the cushion robot in Fig. 8. The rules governing the robot response are given below (similar rules apply in other obstacle scenarios).

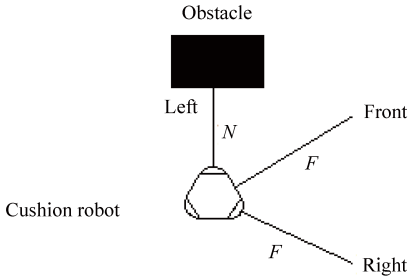

Fig. 8. Obstacle to the left of the cushion robot.

Rule 1: If D_L is N, D_F is F, D_R is F, and A_F is LB, then A_D is TZ.

Rule 2: If D_L is N, D_F is F, D_R is F, and A_F is LS, then A_D is TZ.

Rule 3: If D_L is N, D_F is F, D_R is F, and A_F is Z, then A_D is TZ.

Rule 4: If D_L is N, D_F is F, D_R is F, and A_F is RS, then A_D is TRS.

Rule 5: If D_L is N, D_F is F, D_R is F, and A_F is RB, then A_D is TRB.

C. Fuzzy Inference Mechanism and Defuzzification

Fuzzy inference is the core of the fuzzy algorithm. The steering angle of the cushion robot is influenced by the goal direction and distances to obstacles. This relationship is described by the fuzzy rules, here implemented by the Mamdani fuzzy inference method. To explain the fuzzy inference mechanism, we suppose an input set of $\{D_L = 1.1,\ D_F = 2.3,\ D_R = 3,\ A_F = 15^\circ\}$. According to Fig. 5, the real values $D_L = 1.1$, $D_F = 2.3$, and $D_R = 3$ are mapped to the fuzzy subsets N, F, and F, respectively, and the real value $A_F = 15^\circ$ is mapped to the fuzzy subsets Z and RS. Therefore, fuzzy Rules 3 and 4 are activated. The Mamdani inference method obtains the fuzzy membership of the output. The fuzzy memberships of Rules 3 and 4 inference results are presented in Figs. 9 and 10, respectively. The fuzzy membership of the synthesis inference result is presented in Fig. 11.

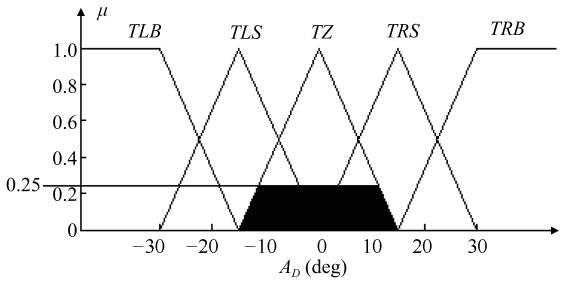

Fig. 9. Inference result of Rule 3.

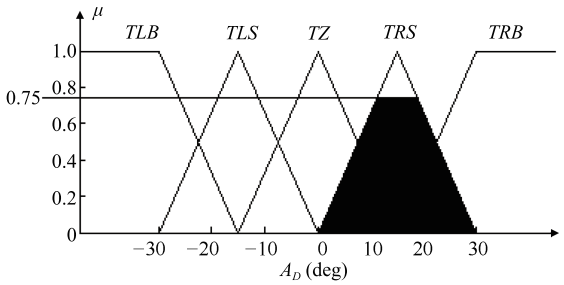

Fig. 10. Inference result of Rule 4.

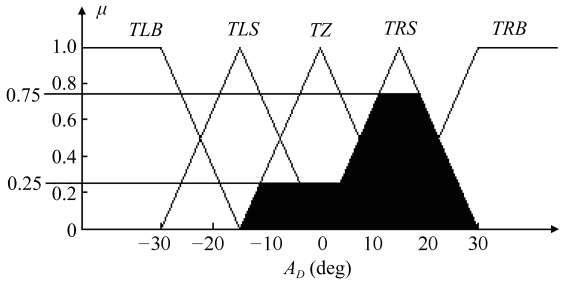

Fig. 11. Synthesis inference result.

Once the fuzzy synthesis inference result is obtained, the inference results are defuzzified by the centroid method (9), and logically summed to give the cushion robot's steering angle A_D.

$$\Delta\theta_d(t) = \frac{\int_{A_D} \mu(A_D) A_D d(A_D)}{\int_{A_D} \mu(A_D) d(A_D)} \tag{9}$$

$$\theta_d(t+1) = \theta_d(t) + \Delta\theta_d(t) \tag{10}$$

where $\Delta\theta_d(t)$ is the clarity value of the steering angle A_D. Inserting this into (10), we get the motion angle $\theta_d(t)$ of obstacle avoidance of the cushion robot, and hence the desired path $X_d(t)$ can be obtained using $\theta_d(t)$.

Remark 2: From the values of the input variables, namely, the robot-obstacle distances (D_F, D_L, and D_R) and the direction angle (A_F), we can determine the fuzzy input variables. The fuzzy rules are determined by searching a collision-free path in trial-and-error simulations, using the triangular and symmetric membership functions. The fuzzy output steering angle of obstacle avoidance A_D is then obtained by the Mamdani fuzzy inference method.

D. Path Planning

Here, we set the motion velocity $v = 0.5\,\text{m/s}$, the initial position at $x(0) = 0\,\text{m}$ and $y(0) = 0\,\text{m}$, and $\theta(0) = \pi/4$ rad. The goal direction and obstacle distances are detected by the ultrasonic sensors of the cushion robot. The resulting fuzzy planned angle $\theta_d(t)$ of obstacle avoidance is shown in Fig. 12. The paths planned in real-time ($X_d(t)$) and computed by the artificial potential field method are compared in Fig. 13.

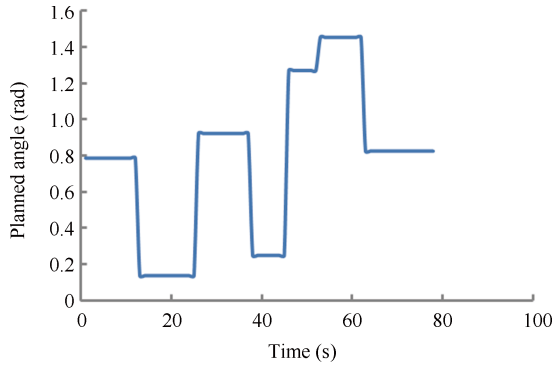

Fig. 12. Planned angle of obstacle avoidance.

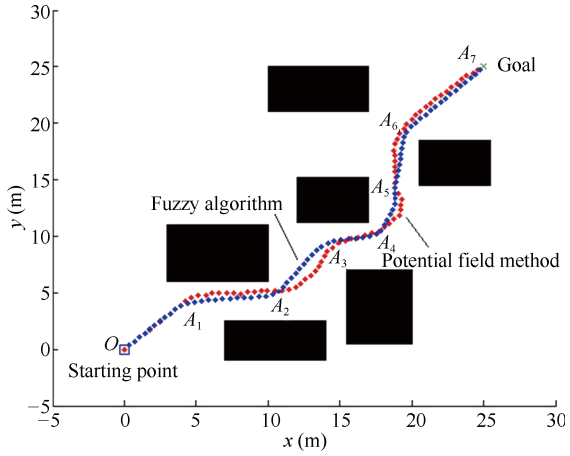

Fig. 13. Motion path of the cushion robot.

Along path OA_1, the planned angle of obstacle avoidance from time $t = 0$ to $t = t_1$ is $\theta_1 = \pi/4$. Thus, we obtain

$$\begin{aligned} x_d(t) &= \cos\theta_1 \times v \\ y_d(t) &= \sin\theta_1 \times v \\ \theta_d(t) &= 0. \end{aligned} \tag{11}$$

Integrating both sides of (11) from 0 to t, the planned path is described by

$$\begin{aligned} x_d(t) &= \cos\theta_1 \times vt \\ y_d(t) &= \sin\theta_1 \times vt \\ \theta_d(t) &= \theta_1. \end{aligned} \tag{12}$$

Likewise, the planned motion path for obstacle avoidance OA_7 is obtained as follows

$$\begin{cases} \begin{cases} x_d(t) = \cos\theta_1 \times vt, & 0 \le t < t_1 \\ x_d(t) = cos\theta_1 \times vt_1 + \cos\theta_2 \times v(t-t_1), & t_1 \le t < t_2 \\ \quad\vdots \\ x_d(t) = \cos\theta_1 \times vt_1 + \cos\theta_2 \times vt_2 + \cdots & \\ \quad + \cos\theta_7 \times v(t-t_6), & t_6 \le t \le t_7 \end{cases} \\ \begin{cases} y_d(t) = \sin\theta_1 \times vt, & 0 \le t < t_1 \\ y_d(t) = \sin\theta_1 \times vt_1 + \sin\theta_2 \times v(t-t_2), & t_1 \le t < t_2 \\ \quad\vdots \\ y_d(t) = \sin\theta_1 \times vt_1 + \sin\theta_2 \times vt_2 + \cdots & \\ \quad + \sin\theta_7 \times v(t-t_6), & t_6 \le t \le t_7 \end{cases} \\ \begin{cases} \theta_d(t) = \frac{\pi}{4}, & 0 \le t < t_1 \\ \theta_d(t) = 0.136, & t_1 \le t < t_2 \\ \quad\vdots \\ \theta_d(t) = 0.823, & t_6 \le t \le t_7. \end{cases} \end{cases} \tag{13}$$

Equation (13) completes the path planning $X_d(t)$. Next, we will design a controller with angular velocity constraints to track the desired path.

Remark 3: A path planning method for the cushion robot is proposed on the basis of fuzzy inference algorithm. The planned motion path is obtained as (11)−(13) when the angle of obstacle avoidance is determined using (9) and (10).

IV. Design of Tracking Controller

Our designed controller tracks the path planned by the cushion robot in an indoor environment under the safety constraints imposed on the angular velocity.

Theorem 1: Considering the error equation (7), if there exist symmetric positive matrices P and Q, as well as matrices S and R, satisfying the following linear matrix inequality (LMI):

$$\begin{bmatrix} S & R & 0 & 0 \\ P & 0 & 0 & 0 \\ 0 & 0 & 0 & \frac{a}{2} \\ 0 & 0 & \frac{a}{2} & 0 \end{bmatrix} \le 0 \tag{14}$$

then the trajectory tracking error $e_1(t)$ and the velocity tracking error $e_2(t)$ are asymptotically stable.

Proof: To prove Theorem 1, we define the Lyapunov function

$$V(t) = \frac{1}{2}e_1^T(t)Pe_1(t) + \frac{1}{2}e_2^T(t)Qe_2(t). \tag{15}$$

The time derivative of $V(t)$ along the tracking error of system (7) is given by

$$\dot{V}(t) = e_1^T(t)Pe_2(t) + e_2^T(t)QK_de_2(t) + e_2^T(t)QK_pe_1(t). \tag{16}$$

Pre-multiply and post-multiply equation (14) by $x^T(t)$ and $x(t)$, respectively. where

$$x^T(t) = \left[e_2^T(t) \; e_1^T(t) \; \left|\ddot{\theta}(t)\right|^T \; 1 \right].$$

We obtain

$$e_2^T(t)Se_2(t) + e_1^T(t)Pe_2(t) + e_2^T(t)Re_1(t) + \frac{a}{2}\left|\ddot{\theta}(t)\right| + \frac{a}{2}\left|\ddot{\theta}(t)\right|^T \leq 0 \tag{17}$$

where

$$S = QK_d, \quad R = QK_p.$$

By (16) and (17), we have

$$\dot{V}(t) \leq -a\left|\ddot{\theta}(t)\right|. \tag{18}$$

From (18), we know that $\dot{V}(t) \leq 0$, implying that $\dot{V}(t) = 0$ with $|\ddot{\theta}(t)| = 0$. Namely, there is a single zero solution in the following set:

$$E = \left\{\ddot{\theta}(t)|\dot{V}(t) = 0\right\} = \left\{\ddot{\theta}(t)|\ddot{\theta}(t) = 0\right\}. \tag{19}$$

Therefore, by LaSalles principle, the trajectory tracking error $e_1(t)$ and the velocity tracking error $e_2(t)$ are asymptotically stable. ■

As the tracking error system (7) is asymptotically stable by Theorem 1, the condition (18) is obtained. Further, using the condition (18), we can get the angular velocity constraints performance in the obstacle avoidance. Therefore, we can state Theorem 2.

Theorem 2: Considering the asymptotically stable error system (7), if there exist symmetric positive matrices P and Q satisfying the following LMI:

$$\begin{bmatrix} -\frac{1}{2}Q & 0 & 0 \\ 0 & -\frac{1}{2}P & 0 \\ 0 & 0 & V(0) + a\left|\dot{\theta}(0)\right| - a^2 \end{bmatrix} \leq 0 \tag{20}$$

the safety of the angular velocity constraints performance (8) is guaranteed under a suitable controller in the form of (6), where.

$$\left|\dot{\theta}(t)\right| \leq a$$

where

$$V(0) = \frac{1}{2}e_1^T(0)Pe_1(0) + \frac{1}{2}e_2^T(0)Qe_2(0).$$

Further, the controller parameter matrices are given by

$$K_d = Q^{-1}S, \quad K_p = Q^{-1}R.$$

Proof: By (18), we obtain

$$\dot{V}(t) \leq -a\left|\ddot{\theta}(t)\right|. \tag{21}$$

Integrating both sides of inequality (21) from 0 to t as

$$\int_0^t \dot{V}(t)dt \leq \int_0^t \left(-a\left|\ddot{\theta}(t)\right|\right)dt \tag{22}$$

we obtain

$$V(t) - V(0) \leq -a\left(\left|\dot{\theta}(t)\right| - \left|\dot{\theta}(0)\right|\right). \tag{23}$$

Inequality (23) can be rewritten as

$$a\left|\dot{\theta}(t)\right| \leq V(0) + a\left|\dot{\theta}(0)\right| - V(t). \tag{24}$$

Pre-multiply and post-multiply equation (20) by $y^T(t)$ and $y(t)$, respectively, where

$$y^T(t) = [\ e_2^T(t) \quad e_1^T(t) \quad 1\ ].$$

We obtain

$$-\frac{1}{2}e_1^T(t)Pe_1(t) - \frac{1}{2}e_2^T(t)Qe_2(t) + V(0) + a\left|\dot{\theta}(0)\right| - a^2 \leq 0. \tag{25}$$

From (15) and (25), it follows that

$$-V(t) + V(0) + a\left|\dot{\theta}(t)\right| \leq a^2. \tag{26}$$

Combining (24) and (26) leads to

$$a\left|\dot{\theta}(t)\right| \leq a^2. \tag{27}$$

Hence, we have

$$\left|\dot{\theta}(t)\right| \leq a.$$

Furthermore, by Theorem 1, the controller that ensures safe angular velocity is given by

$$K_d = Q^{-1}S, \quad K_p = Q^{-1}R.$$

The tracking safe angular velocity constraints performance is satisfied. ■

Remark 4: A new tracking control method with angular velocity constraints performance is proposed, and the safe angular velocity can be obtained from the common Lyapunov function $V(t)$. Therefore, when the fuzzy obstacle avoidance angle $\theta_d(t)$ of the cushion robot is determined, the motion angular velocity is restricted to the safe range. Our simple method avoids the need for a saturation function with compensation [19], [20], or a complex BLF for state variable constraints [21].

Remark 5: The matrices P, Q, S and R can be obtained by solving the LMIs (14) and (20). Thus the controller parameters can be determined as $K_d = Q^{-1}S$, $K_p = Q^{-1}R$ through Theorem 2.

Remark 6: The asymptotically stable condition (14) of tracking error system is given in Theorem 1. Using the condition (18) of Theorem 1, the angular velocity constraints performance (8) is gotten in Theorem 2. The significant feature of the proposed controller (6) is its ability to directly restrict the motion angular velocity.

V. Simulation Results

In this section, the proposed tracking control algorithm with fuzzy path planning and safety constraints on the angular velocity is verified in a cushion robot. The physical parameter values of the cushion robot are given in Table I.

TABLE I
PHYSICAL PARAMETERS

Parameter	Value
Mass M	15 kg
Maximum load m	75 kg
Distance l	0.45 m
Inertia of mass I_0	0.67 kg·m^2
Maximum velocity v	0.6 m/s
Maximum angular velocity	1.8 rad/s

The user load parameters are $m = 60$ kg and $r_0 = 0.1$ m. To ensure the user's safety, we set $a = \pi/6$ rad/s, i.e., $\left|\dot{\theta}(t)\right| \leq \pi/6$ rad/s. Solving the inequalities (14) and (20), we obtain the controller parameters $K_p = \text{diag}\{-20.59, -25.34, -4.59\}$ and $K_d = \text{diag}\{-5.18, -5.18, -10.02\}$. The simulation results are presented in the following figures.

Figs. 14 and 15 plot the trajectories of the x and y positions, respectively. Real-time tracking by the cushion robot conformed to the planned obstacle avoidance path (see Fig. 16). This confirms the asymptotic stability of the tracking error state equation. Fig. 17 plots the motion angular velocity of obstacle avoidance. The proposed control method guaranteed an angular velocity within the safe operating range, demonstrating that the cushion robot can be safely adopted by users. These simulation results confirm that the controller (6) effectively realizes path tracking while properly constraining the angular velocity performance.

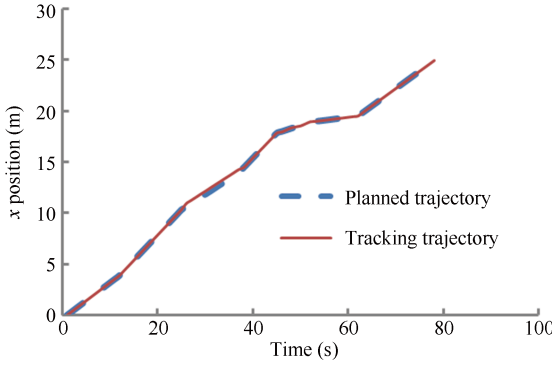

Fig. 14. Trajectory tracking of x position.

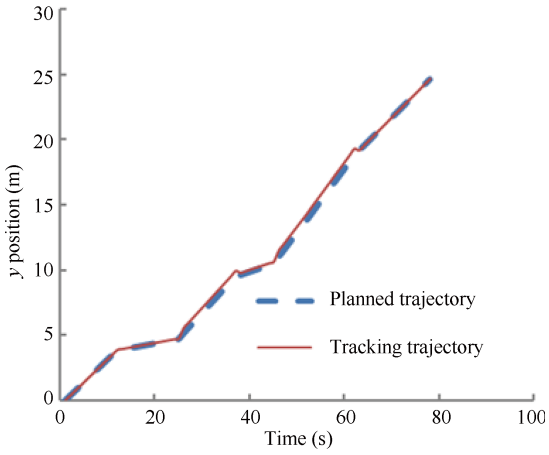

Fig. 15. Trajectory tracking of y position.

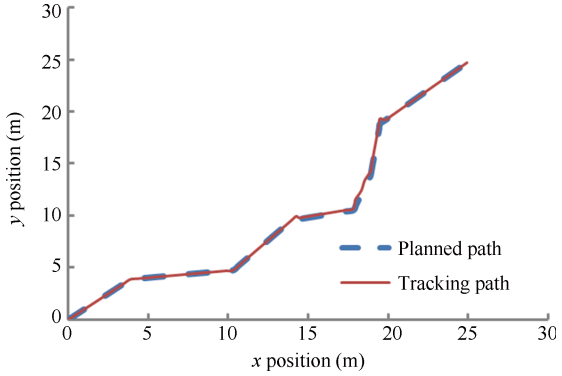

Fig. 16. Path tracking.

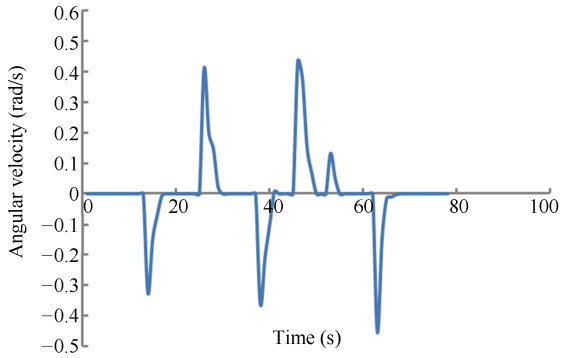

Fig. 17. Safe motion angular velocity.

Next, we examine the user-dependent tracking performance of the cushion robot. In this simulation, we vary the user's load as $m = 50$ kg and apply the same K_p, K_d and initial values to the controller (6). The simulation results are shown below.

Fig. 18 plots the tracking errors in the x and y positions. A few tracking errors appear in the 25−60 s range, but these low amplitude errors have little effect on the trajectory tracking. The motion angular velocity of obstacle avoidance is shown in Fig. 19. Again, the cushion robot constrains the angular velocity within the safe range for the user.

To verify the effectiveness of the tracking control under angular velocity constraints, we compared the performance of our proposed control system with that of unconstrained tracking control.

In these comparative simulations, the parameter matrices $K_p = \text{diag}\{-51, -55, -21\}$ and $K_d = \text{diag}\{-16, -28, -13\}$ in the controller (6) were adjusted manually and iteratively until the trajectory tracking began from the same initial values in both cases. The simulation results are presented in the following figures.

Fig. 20 plots the tracking performance of the cushion robot along the planned obstacle avoidance path. Evidently, the unconstrained controller achieves asymptotic stability and good path tracking, but the angular velocity of the cushion robot

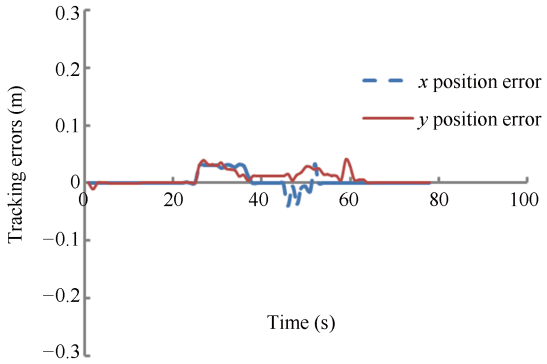

Fig. 18. Tracking errors.

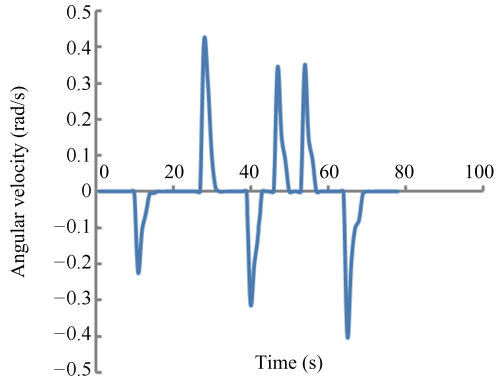

Fig. 19. Safe motion angular velocity.

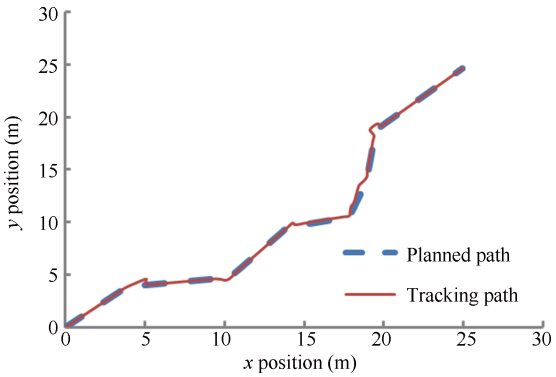

Fig. 20. Path tracking.

exceeded the prescribed safe range during obstacle avoidance tasks (see Fig. 21). Therefore, constraining the angular velocity in the controller is an essential part of the cushion robot design.

VI. Experiment Results

This section shows an experiment in which the cushion robot with the proposed fuzzy path planning and angular velocity constraints realizes safe path tracking.

The physical parameter values of the cushion robot are given in Table I. A camera, which records the real-time position of the robot and feeds these values back to the controller, is installed on the roof. The position includes the x and y positions, and the planned angle of obstacle avoidance $\theta_d(t)$. The camera frame rate is 30 fps. OpenCV is used to recognize and output the robot position and posture during the path tracking.

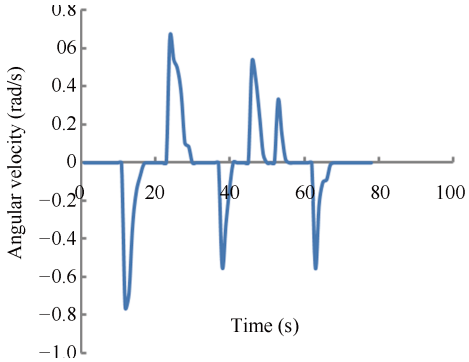

Fig. 21. Motion angular velocity.

To clarify the performance of obstacle avoidance and tracking control, two obstacles are put on the floor and a load (instead of a user) is put on one side of the robot to reflect the load change and center of gravity shift. The experimental environment is shown in Fig. 22. The resulting fuzzy planned angle $\theta_d(t)$ of obstacle avoidance is shown in Fig. 23.

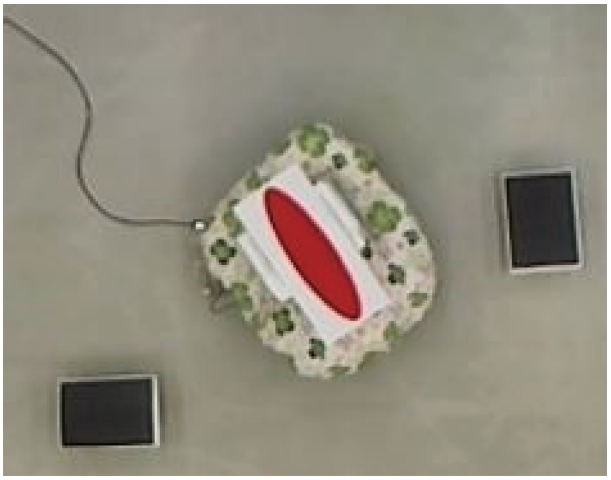

Fig. 22. Experimental environment.

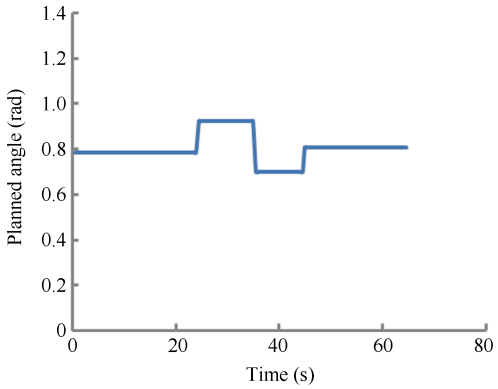

Fig. 23. Planned angle of obstacle avoidance.

Therefore, the planned collision-free motion path is obtained as follows.

$$
\begin{cases}
\begin{cases}
x_d(t) = \cos\theta_1 \times vt, & 0 \le t < 24 \\
x_d(t) = \cos\theta_1 \times 24v \\
\qquad + \cos\theta_2 \times v(t-24), & 24 \le t < 35 \\
x_d(t) = \cos\theta_1 \times 24v + \cos\theta_2 \times 11v \\
\qquad + \cos\theta_3 \times v(t-35), & 35 \le t \le 45 \\
x_d(t) = \cos\theta_1 \times 24v + \cos\theta_2 \times 11v \\
\qquad + \cos\theta_3 \times 10v + \cos\theta_4 \times v(t-45), & 45 \le t \le 65
\end{cases} \\
\begin{cases}
y_d(t) = \sin\theta_1 \times vt, & 0 \le t < 24 \\
y_d(t) = \sin\theta_1 \times 24v + \sin\theta_2 \times v(t-24), & 24 \le t < 35 \\
y_d(t) = \sin\theta_1 \times 24v + \sin\theta_2 \times 11v \\
\qquad + \sin\theta_3 \times v(t-35), & 35 \le t < 45 \\
y_d(t) = \sin\theta_1 \times 24v + \sin\theta_2 \times 11v \\
\qquad + \sin\theta_3 \times 10v + \sin\theta_4 \times v(t-45), & 45 \le t \le 65
\end{cases} \\
\begin{cases}
\theta_d(t) = \frac{\pi}{4}, & 0 \le t < 24 \\
\theta_d(t) = 0.921, & 24 \le t < 35 \\
\theta_d(t) = 0.701, & 35 \le t < 45 \\
\theta_d(t) = 0.806, & 45 \le t \le 65
\end{cases}
\end{cases} \tag{28}
$$

We carry out two tests: one without any load $m = 0\,\text{kg}$, and the other with $m = 15\,\text{kg}$. The experimental results are presented below.

Figs. 24 and 25 plot real-time tracking by the cushion robot for the planned obstacle avoidance path, respectively. A few tracking errors appear around the corner, but these low amplitude errors have little effect on the path tracking. The driving input forces f_1, f_2, and f_3 on the three omnidirectional wheels are shown in Figs. 26 and 27, respectively. The motion angular velocity of obstacle avoidance is shown in Figs. 28 and 29. These experimental results confirm that the controller (6) effectively realizes path tracking with or without a load while properly constraining the angular velocity performance. Therefore, the cushion robot with the proposed fuzzy path planning and safe angular velocity constraints controller is reliable for assisting the in-room movement of users.

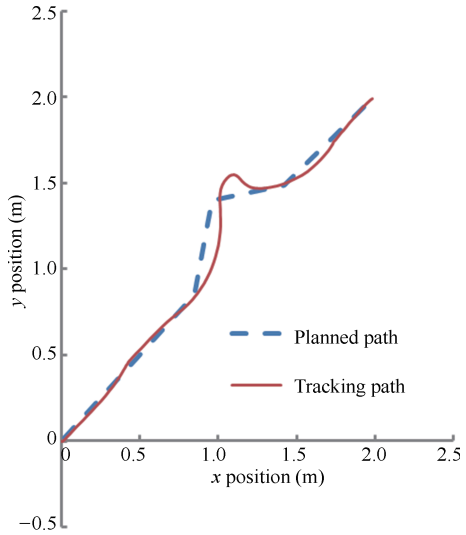

Fig. 24. Path tracking ($m = 0\,\text{kg}$).

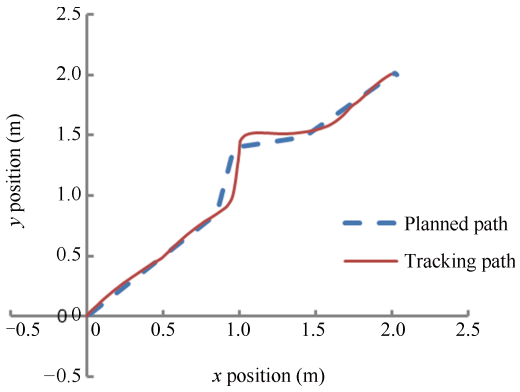

Fig. 25. Path tracking ($m = 15\,\text{kg}$).

VII. Conclusions

This paper proposed a new tracking control approach for

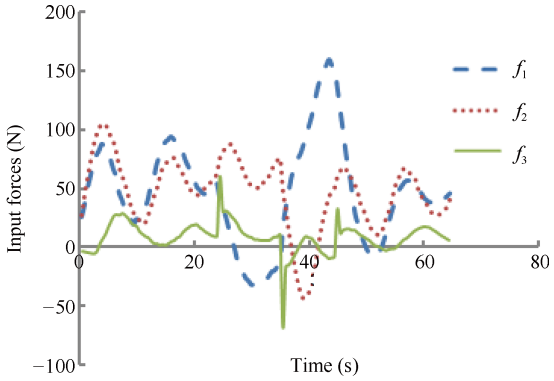

Fig. 26. Control input forces ($m = 0\,\text{kg}$).

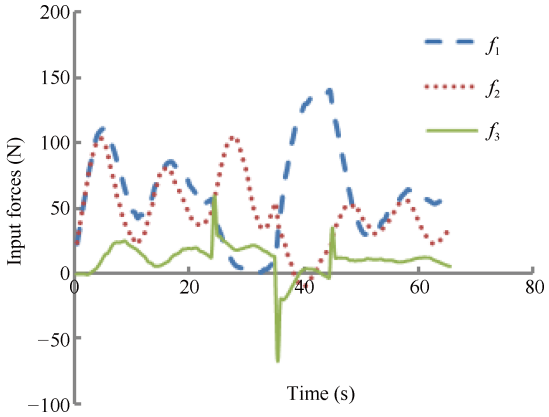

Fig. 27. Control input forces ($m = 15\,\text{kg}$).

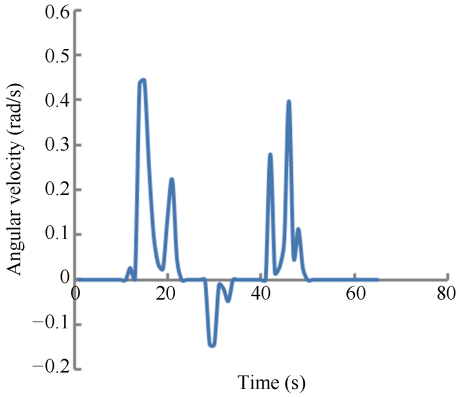

Fig. 28. Motion angular velocity ($m = 0\,\text{kg}$).

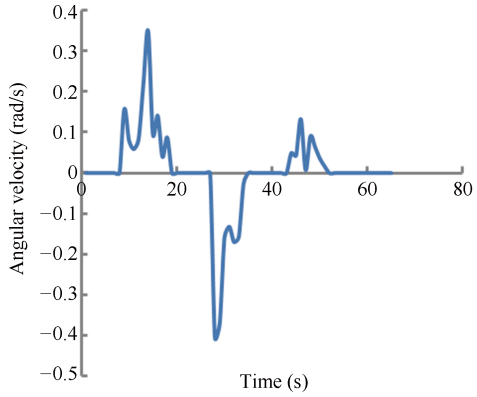

Fig. 29. Motion angular velocity ($m = 15\,\text{kg}$).

a cushion robot, which constrains the angular velocity of obstacle avoidance within a safe range for elderly and/or infirm users. Safe motion of the cushion robot is guaranteed by fuzzy path planning of the obstacle avoidance method. The obtained tracking controller stabilizes the robot using a common Lyapunov function, and properly constrains the angular velocity performance. Such constraints have not been imposed in previous path planning studies of wheeled service robots. The effectiveness of safe turning by fuzzy path planning and tracking control was confirmed in simulation and experiment results. The proposed method was implemented in a cushion robot, but is expected to be equally applicable to other wheeled service robots.

REFERENCES

[1] L. Z. Pan, A. G. Song, S. L. Duan, and B. G. Xu, "Robot-assisted humanized passive rehabilitation training based on online assessment and regulation," *Bio-Med. Mater. Eng.*, vol. 26, no. S1, pp. S655−S664, Sep. 2015.

[2] Z. Guo, H. Y. Yu, and Y. H. Yin, "Developing a mobile lower limb robotic exoskeleton for gait rehabilitation," *J. Med. Devices*, vol. 8, no. 4, Article ID 044503, Aug. 2014.

[3] S. Mohammed, Y. Amirat, and H. Rifai, "Lower-limb movement assistance through wearable robots: State of the art and challenges," *Adv. Robot.*, vol. 26, no. 1−2, pp. 1−22, Apr. 2012.

[4] D. Zanotto, Y. Akiyama, P. Stegall, and S. K. Agrawal, "Knee joint misalignment in exoskeletons for the lower extremities: Effects on user's gait," *IEEE Trans. Robot.*, vol. 31, no. 4, pp. 978−987, Aug. 2015.

[5] P. Sun and S. Y. Wang, "Redundant input safety tracking for omnidirectional rehabilitative training walker with control constraints," *Asian J. Control*, vol. 19, no. 1, pp. 116−130, Jan. 2017.

[6] R. P. Tan, S. Y. Wang, and Y. L. Jiang, "Motion control of a cushion robot considering load change and center of gravity shift," *J. Syst. Des. Dyn.*, vol. 6, no. 5, pp. 740−753, Dec. 2012.

[7] Q. Liu, D. Liu, W. Meng, Z. D. Zhou, and Q. S. Ai, "Fuzzy sliding mode control of a multi-DOF parallel robot in rehabilitation environment," *Int. J. Human. Robot.*, vol. 11, no. 1, Article ID 1450004, Apr. 2014.

[8] W. He, S. S. Ge, Y. N. Li, E. Chew, and Y. S. Ng, "Neural network control of a rehabilitation robot by state and output feedback," *J. Intell. Robot. Syst.*, vol. 80, no. 1, pp. 15−31, Oct. 2015.

[9] J. F. Zhang, Y. M. Dong, C. J. Yang, Y. Geng, Y. Chen, and Y. Yang, "5-Link model based gait trajectory adaption control strategies of the gait rehabilitation exoskeleton for post-stroke patients," *Mechatronics*, vol. 20, no. 3, pp. 368−376, Aug. 2010.

[10] P. Sun and S. Y. Wang, "Redundant input guaranteed cost non-fragile tracking control for omnidirectional rehabilitative training walker," *Int. J. Control Automat. Syst.*, vol. 13, no. 2, pp. 454−462, Apr. 2015.

[11] S. Dale, C. Rusu, A. Bara, and E. Szoke, "Fuzzy based reactive controller for a small mobile robot platform," *J. Comp. Sci. Control Syst.*, vol. 5, no. 1, pp. 89−94, May 2012.

[12] D. W. Kim, T. A. Lasky, and S. A. Velinsky, "Autonomous multi-mobile robot system: simulation and implementation using fuzzy logic," *Int. J. Control Autom. Syst.*, vol. 11, no. 3, pp. 545−554, Jun. 2013.

[13] V. Agarwal, "Trajectory planning of redundant manipulator using fuzzy clustering method," *Int. J. Adv. Manuf. Technol.*, vol. 61, no. 5−8, pp. 727−744, Jul. 2012.

[14] Z. Y. Zhou, Z. G. Zhang, and X. W. Luo, "A fuzzy path preview algorithm for the rice transplanting robot navigation system," *J. Softw.*, vol. 9, no. 4, pp. 881−888, Apr. 2014.

[15] P. K. Mohanty and D. R. Parhi, "Path planning strategy for mobile robot navigation using MANFIS controller," in *Proceedings of the International Conference on Frontiers of Intelligent Computing: Theory and Applications (FICTA) 2013*, S. C. Satapathy, S. K. Udgata, and B. N. Biswal, Eds. Switzerland: Springer, 2014, pp. 353−361.

[16] Y. L. Jiang, S. Y. Wang, K. Ishida, Y. Kobayashi, and M. G. Fujie, "Directional control of an omnidirectional walking support walker: adaptation to individual differences with fuzzy learning," *Adv. Robot.*, vol. 28, no. 7, pp. 479−485, Jan. 2014.

[17] Y. M. Li, S. C. Tong, and T. S. Li, "Adaptive fuzzy output-feedback control for output constrained nonlinear systems in the presence of input saturation," *Fuzzy Sets Syst.*, vol. 248, pp. 138−155, Aug. 2014.

[18] J. P. Kolhe, M. Shaheed, T. S. Chandar, and S. E. Talole, "Robust control of robot manipulators based on uncertainty and disturbance estimation," *Int. J. Robust Nonlinear Control*, vol. 23, no. 1, pp. 104−122, Jam. 2013.

[19] M. Yue, G. Q. Wu, S. Wang, and C. An, "Disturbance observer-based trajectory tracking control for nonholonomic wheeled mobile robot subject to saturated velocity constraint," *Appl. Artif. Intell.*, vol. 28, no. 8, pp. 751−765, Oct. 2014.

[20] J. Moreno-Valenzuela and V. Santibáñez, "Robust saturated PI joint velocity control for robot manipulators," *Asian J. Control*, vol. 15, no. 1, pp. 64−79, Jan. 2013.

[21] B. Niu and J. Zhao, " Brief Paper-output tracking control for a class of switched non-linear systems with partial state constraints," *IET Control Theory Appl.*, vol. 7, no. 4, pp. 623−631, Mar. 2013.

Ping Sun received the Ph.D. degree in control theory and applications from Northeastern University, China, in 2006. She is currently an Associate Professor at the School of Information Science and Engineering, Shenyang University of Technology, China. Her research interests include walking rehabilitation robots control and nonlinear systems control.

Zhuang Yu received the bachelor degree in measurement and control technology and instrumentation from Tianjin University of Science and Technology, China, in 2013. Currently, he is pursuing the master degree at Shenyang University of Technology in control engineering. His research interests include life service robots path planning.